Structural and Dielectric Properties of Sol-Gel Derived PLZT (x/60/40)

S.R. SHANNIGRAHI & R.N.P. CHOUDHARY

Department of Physics and Meteorology, Indian Institute of Technology, Kharagpur- 721 302, India

Abstract. Polycrystalline samples of $(Pb_{1-z}La_z)(Zr_{0.60}Ti_{0.40})_{1-z/4}O_3$ (where $z = 0.00$, 0.05, 0.09, 0.12, 0.14 mol %) (abbreviated as PLZT) were synthesized through acetate-alkoxide sol-gel route. The formation and existence of different crystallographic phases as a function of z was checked through X-ray, TEM, SEM and dielectric studies. The diffuse phase transition (DPT) was observed in PLZT with higher concentration of La (i.e., for $z = 0.00$ to 0.12), but for $z = 0.14$, the compound did not show any phase transition.

Keywords: sol-gel, XRD, diffuse phase transition, ferroelectrics, PLZT

1. Introduction

Since the discovery of ferroelectricity in $BaTiO_3$ [1] in 1945, a large number of materials of different structural families (e.g., perovskite, tungsten bronze (TB), spinel etc.) have been studied in search of new materials for device applications. Among all the oxides studied so far, some compounds and/or solid solutions of perovskite family of a general formula ABO_3 (A = mono or divalent; B = tri to pentavalent ions) have been found useful for different electronic devices. Some lead based perovskite compounds namely, $PbTiO_3, PbZrO_3, Pb(ZrTi)O_3, Pb(MgNb)O_3$ etc., have special positions in the field of ferroelectrics. Lead zirconate titanate, $Pb(ZrTi)O_3$ (abbreviated as PZT), solid-solution of ferroelectric $PbTiO_3 (T_c = 490°C)$ and antiferroelectric $PbZrO_3$ $(T_c = 230°C)$, with varying Zr/Ti ratios has wide industrial applications (e.g., computer memory and display, transducer, actuator, pyroelectric detector etc.) [2–8]. It is now well established that the variation of Zr/Ti ratio and the suitable substitutions at A and/or B-sites influence the physical properties and/or device parameters of PZT to a great extent [9]. Most of the previous studies have been done on solid-solutions of PZT with Zr/Ti = 65/35 doped with 8% La (at Pb-site) near morphotropical phase boundary (MPB).

Extensive or up-to-date literature survey on PZT and/ or PLZT reveals that effect of rare-earth ions on the physical properties of PZT with Zr/Ti = 60/40 has not been studied much. Further, the substitution of these ions at Pb-sites of PZT provides phase transition of diffuse type. In view of the above, we have extensively studied the effect of rare-earth ions substitution (at Pb-sites) on the structural, piezoelectric, pyroelectric and ferroelectric properties of PZT. In this paper, we report the effect of La substitution on the above physical properties of PZT (x/60/40) (where $z = 0.00$, 0.05, 0.09, 0.12, 0.14).

2. Experimental Details

Polycrystalline samples of $(Pb_{1-z}La_z)$ $(Zr_{0.60}Ti_{0.40})_{1-z/4}O_3$ (denoted as PLZT) were synthesized using the following precursors: lead acetate trihydrate $Pb(CH_3COO)_2 \cdot 3H_2O$ (99.9%, M/s. E. Merck, Germany), lanthanum acetate hexahydrate $La(CH_3COO)_3 \cdot 6H_2O$ (99.5%, M/s. B.D.H., UK), zirconium propoxide $Zr(C_3H_7O)_4$ (70 wt % in iso-propanol, M/s. Fluka, Switzerland) and titanium isopropoxide $Ti[(CH_3)_2CHO]_4$ (>97% Ti, M/s. E. Merck, Germany) in a required stoichiometry. Glacial acetic acid and distilled water were used as solvents.

Ethylene glycol was used as an additive in order to get monolithic gel. First of all, lead acetate and lanthanum acetate were dissolved separately in acetic acid in the ratio of 2 gm of salt in 1 ml acid, and were heated at 110°C for half an hour to remove the water content, and then cooled down to 80°C. These two solutions were mixed in a beaker and stirred. During stirring zirconium propoxide followed by titanium isopropoxide were added in the mixture. Ethylene glycol was then added in the proportion of 1 ml to 10 g of lead acetate in the solution. The initial reaction had to be completed before the glycol was added since residual titanium isopropoxide, and zirconium propoxide alcolyzes with ethylene glycol to form a condensed solid. A small amount of distilled water was added to get the final sol. The sol was kept at 60°C for 24 h to get the clear transparent gel. The gel was dried at 100°C in an oven for 72 h and then a light brown powder was obtained. The DTA analysis of the oven-dried gel was carried out in a Shimadzu DT-40 thermal analyser at a heating rate of $5°C \, min^{-1}$ (sensitivity of $8 \mu V \cdot cm^{-1}$).

The oven dried powdered gel was calcined at 550°C for 15 h. The powder was cold pressed into pellets at a pressure of 6×10^6 Pa using a hydraulic press. The time and temperature used for sintering the pellets were 60 h and 1200°C for La-doped PZT and 7 h and 1300°C for pure PZT samples respectively. In order to prevent PbO loss and maintain the stoichiometry of the compounds during sintering, an equilibrium PbO vapour pressure was established with $PbZrO_3$ as setter and placing everything in the covered platinum crucible. The density of the sintered pellets was measured using the Archimedes' method, and was found to be 97–98% of the theoretical density.

The formation and quality of the PLZT compounds were checked by X-ray diffraction (XRD) technique. The XRD data were collected using a powder diffractometer (Philips PW 1877) having Cu target (CuK_α radiation ($\lambda = 0.15418 \, nm$)) in a wide range of Bragg angles 2θ ($20° \leq 2\theta \leq 60°$) with a scanning rate of $3° \, min^{-1}$ on powders as well as on sintered pellet samples. Microstructures of the samples were taken by TEM (JEM 200 CX) and SEM (CAMSCAN 180) at different magnifications.

A high-purity silver-paste was then painted on the flat polished surfaces of the sintered pellets to act as electrode and then dried at 100°C before taking any electrical measurements. The dielectric constant (ε) and tangent loss ($\tan\delta$) of the samples were obtained using a GR 1620 AP capacitance measuring assembly with a three-terminal sample holder as a function of frequency ($400 - 10^4$ Hz) at room temperature and temperature (30–400°C) at 10^4 Hz.

The variation of remanent polarisation (P_r) and coercive field (E_c) of the samples was recorded at 50 Hz with an ac field of $20 \, kV \cdot cm^{-1}$ using a laboratory-modified Sawyer and Tower circuit.

3.   Results and Discussion

Figure 1 shows the DTA curve of the oven-dried sample for $z = 0.00$. The curve showed two exothermic peaks at the temperatures 300 and 481°C. The first peak was attributed to oxidation of the alkyl groups present in the gel because of an incomplete polycondensation reaction [10]. The second one was due to the crystallization of the compound. This was evident from our X-ray and TEM analysis. Although the thermal analyses show that the reaction was completed at 481°C, the final calcination was performed at 550°C to ensure the removal of any remanent volatiles.

The room temperature single and sharp X-ray diffraction (XRD) patterns of the calcined powders and sintered pellets of PLZT samples, which are different from those of the ingredients, show the formation of single-phase compounds. All the reflection peaks were indexed and lattice parameters of the PLZT samples were determined and refined using the least-squares refinement method of a computer package (PowdMult). Compared to PZT, a small shift in peak position of XRD patterns was
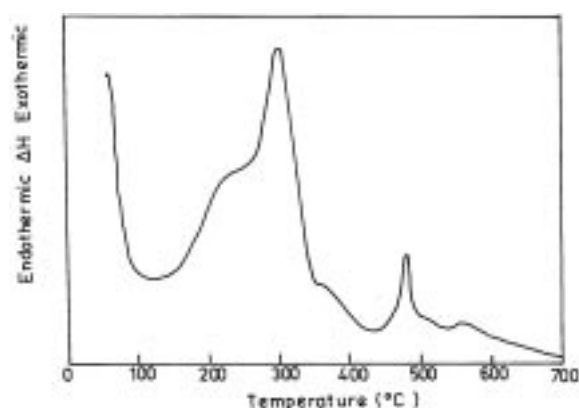

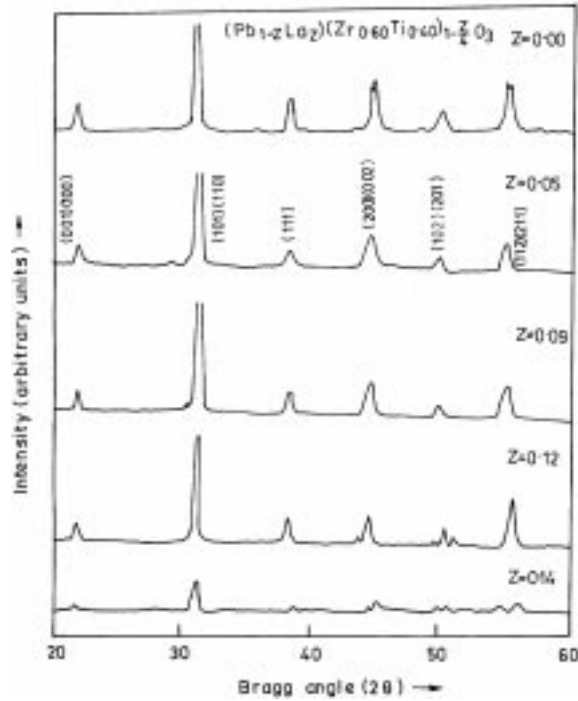*Fig. 1.* DTA curve of the oven dried PZT.

Fig. 2. Comparison of XRD of the PLZT.

observed (Fig. 2), which suggested that the basic crystal structure of PZT have not been affected by the incorporation of the La^{3+} ions. A small shift in the peak positions has provided a small change in the lattice parameters (Table 1). The PLZT compounds for $z = 0.0$ to 0.05 belong to the rhombohedral (R), for $z = 0.07$ to 0.10 tetragonal (T), $z = 0.12$ belongs to mixed $(T + C)$ and $z = 0.14$ belongs to cubic (C) phase at room temperature.

Figure 3(a) shows transmission electron micrographs of the calcined PLZT powders. Figure 3(a) is selected area electron diffraction (SAED) pattern of Fig. 3. The interplanar spacing (d_{hkl}) obtained from the TEM and XRD patterns are very much compar-

able (Table 2) that confirms the presence of crystalline phase of the materials. It is also observed from TEM that the particles of the PLZT powders are spherical. It can be seen that the particles are uniformly distributed through out the sample. The average particle size of the sample increases with the increase of z. From the SEM micrographs of PLZT (Fig. 4), it is clear that the grains of the samples are uniformly distributed on the surface of the sintered samples. The grain size decreases with the increase of La^{3+}. The grains are nearly spherical and in the range of 4.5–5 μm.

The variation of ε and $\tan\delta$ as a function of frequency $(400 - 10^4 \text{ Hz})$ at room temperature is shown in the Fig. 5. They are almost independent of frequency above 1 kHz. Figures 6 and 7 show the variation of ε and $\tan\delta$ with temperature at 10^4 Hz for all five different compositions (z) of La. In normal ferroelectrics, the values of ε increase sharply with increasing temperature up to a temperature, called transition (T_c), and then it decreases. But in our PLZT samples, the dielectric peak is found broadened with increasing z. The broadening of the dielectric peaks and the decreasing of peak value of dielectric constant (ε_{max}) may be attributed to inhomogeneity and substitution disordering or fluctuation in the samples. It is also seen that the dielectric peaks shift towards the higher temperature side with decreasing lanthanum mole percent (Table 3) [11].

In order to study the effect of z on the broadening of dielectric peaks and to calculate the degree of disordering in the samples, we have used the following expression [12]

$$\left(\frac{1}{\varepsilon} - \frac{1}{\varepsilon_{max}}\right) \propto (T - T_c)^{\gamma}$$

where ε is dielectric constant at temperature T, ε_{max} is its maximum value at T_c and γ is the measure of diffuseness. The value of γ (diffusivity) calculated

Table 1. Comparison of cell parameters, density, grain size and particle size of PLZT from XRD, SEM and TEM [*T*: tetragonal, *C*: cubic]

z	0.0	0.05	0.09	0.12	0.14
a (Ao)	4.133(*R*)	4.068(*R*)	4.100(*T*)	4.032(*T*)	4.080(*C*)
				4.207(*C*)	
c (Å)	—	—	4.140	4.077	—
α (deg.)	89.6	89.7	—	—	—
d (gm.cc^{-1})	7.51	7.69	7.42	7.66	7.51
Av. Grain size (SEM) (μ m)	5.0	4.9	4.6	4.6	4.5
Av. Particle size (TEM) (Å)	150	220	240	250	280

$z = 0.00$ 1mm = 55Å

1mm = 55 Å $z = 0.05$

$z = 0.09$ 1mm = 59Å

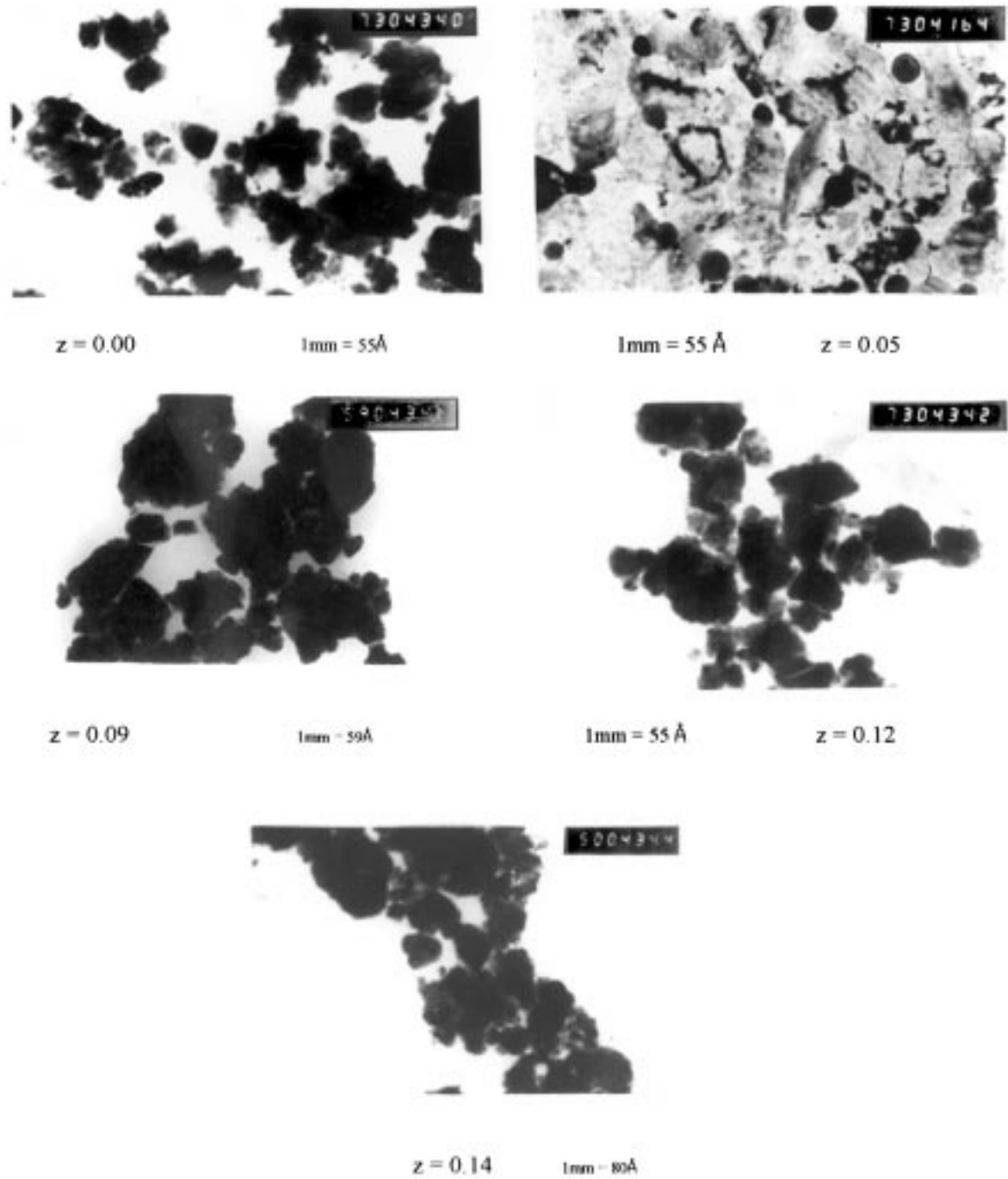1mm = 55 Å $z = 0.12$

$z = 0.14$ 1mm = 80Å

Fig. 3(a). TEM micrographs.

from Fig. 8 was found to be between 1 (for normal ferroelectrics) and 2 (completely disordered ferroelectrics), which confirms the diffuse phase transition in the materials. From Fig. 6, it is clear that the value of maximum dielectric constant (ε_{max}) decreases and/or broadening in peaks increases with
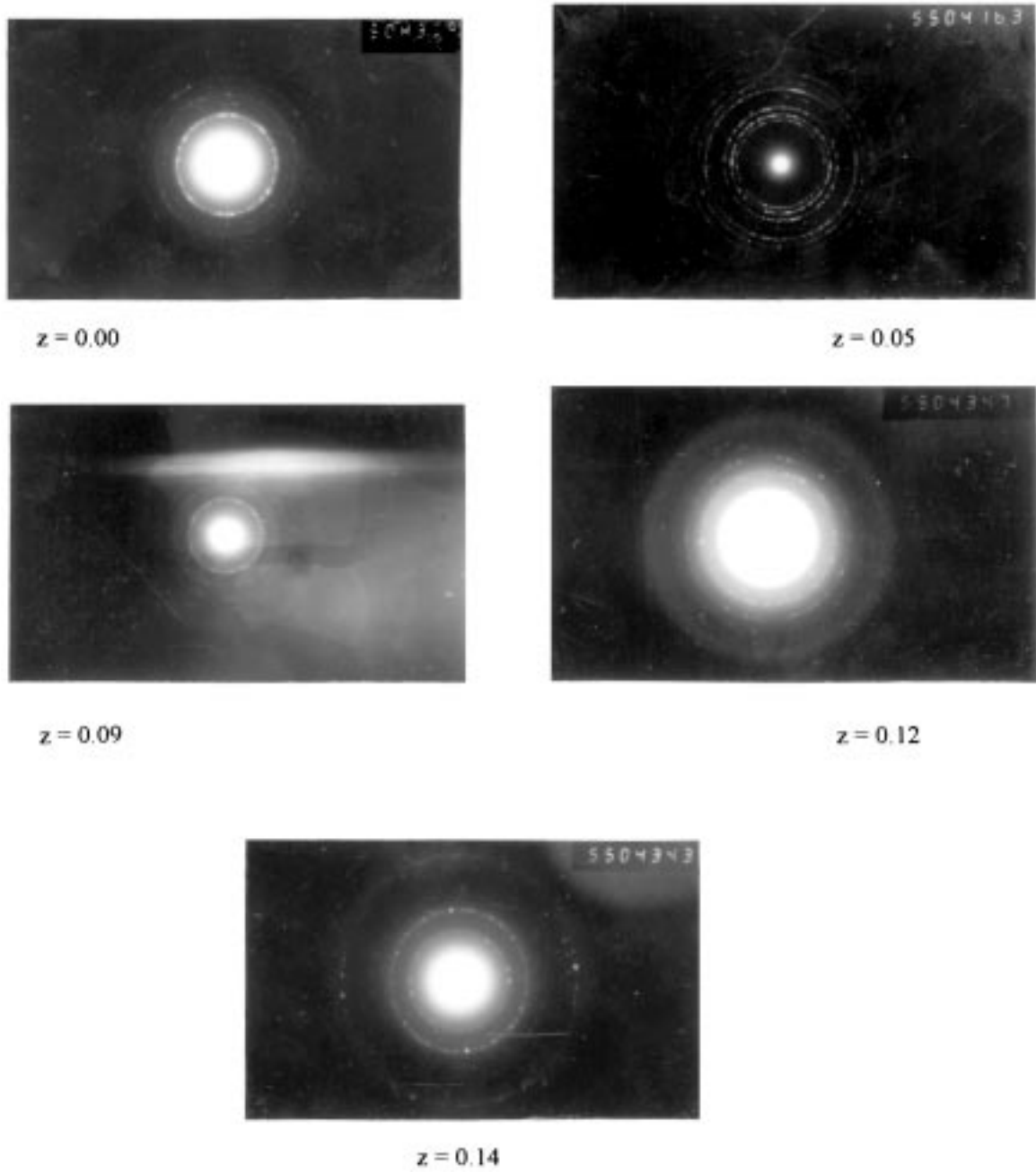
z = 0.00

z = 0.05

z = 0.09

z = 0.12

z = 0.14

Fig. 3(b). Diffraction pattern of PLZT.

increasing doping concentration of La^{3+}. From the calculated value of diffusivity (Table 3), it is also clear that substitution disordering increases with increasing La content in PLZT, and hence for $z = 0.14$ dielectric peak vanishes. It is observed that the reciprocal of dielectric constant is a linear function

Table 2. Comparison of some interplanar spacing d (in Å) measured from XRD (d_{XRD}) and TEM (d_{TEM}) of PLZT

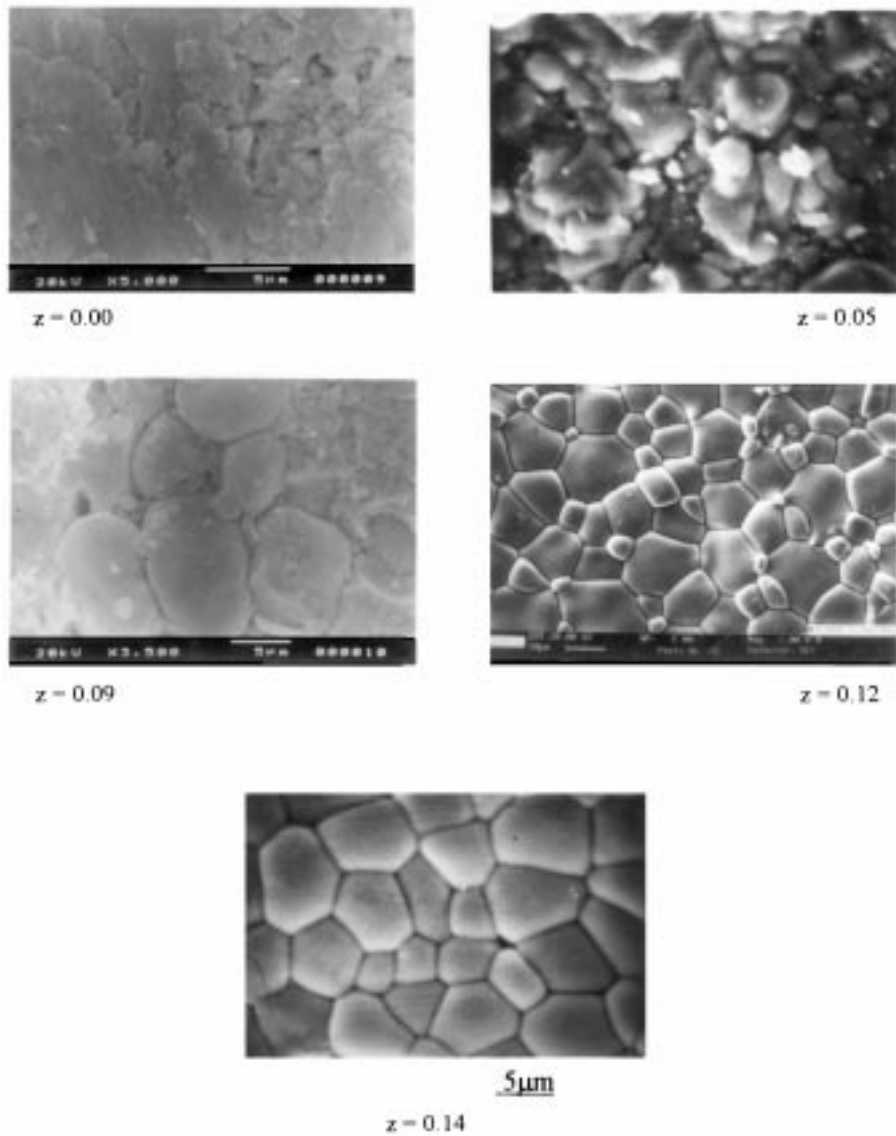| z	0.0		0.05		0.09		0.12		0.14	
h k l	d_{XRD}	d_{TEM}	d_{XRD}	d_{TEM}	d_{XRD}	d_{TEM}	d_{XRD}	d_{TEM}	d_{XRD}	d_{TEM}
0 0 1	4.133	—	4.068	—	4.143	—	4.077	—	4.114	—
1 0 1	2.915	—	2.883	—	2.912	2.927	2.867	—	2.894	—
1 1 1	2.382	—	2.360	—	2.374	2.376	2.350	—	2.356	2.341
2 0 0	2.066	—	2.034	1.993	2.051	2.091	2.036	1.977	2.045	—
2 0 1	1.844	1.839	1.823	—	1.848	—	1.821	—	1.667	1.652
2 1 1	1.683	1.677	1.667	1.672	1.675	1.685	1.661	1.674	1.664	—

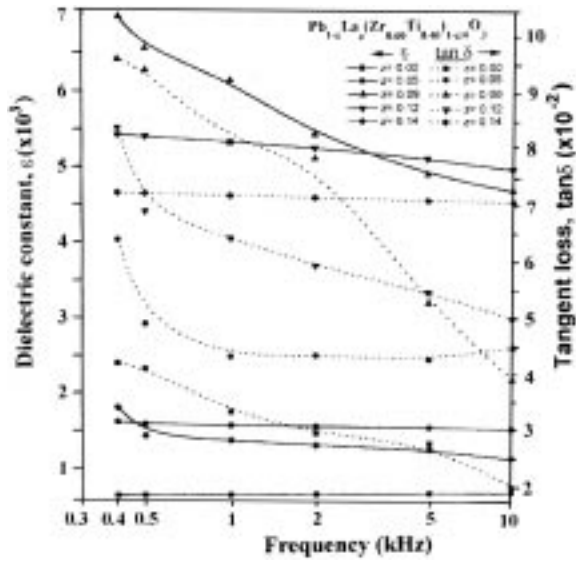*Fig. 4*. SEM micrograph of PLZT.

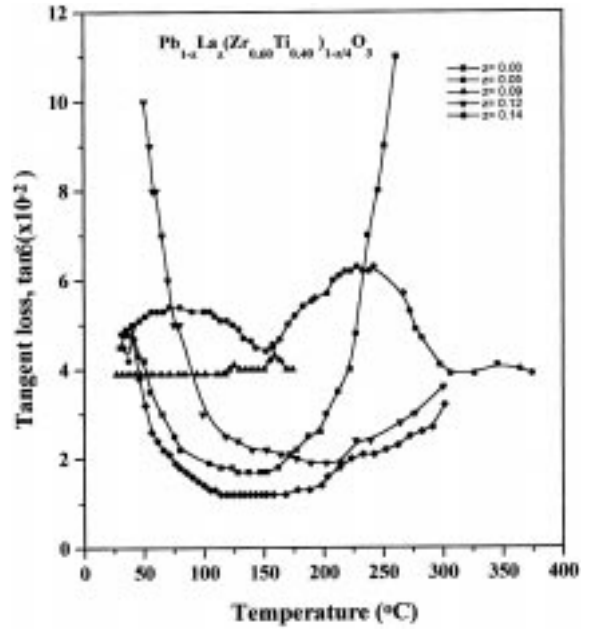*Fig*. 5. Variation of dielectric constant (ε) and tangent loss (tanδ) of PLZT with frequency at room temperature.

Fig. 7. Variation of tangent loss (tanδ) of PLZT with temperature at 10^4 Hz.
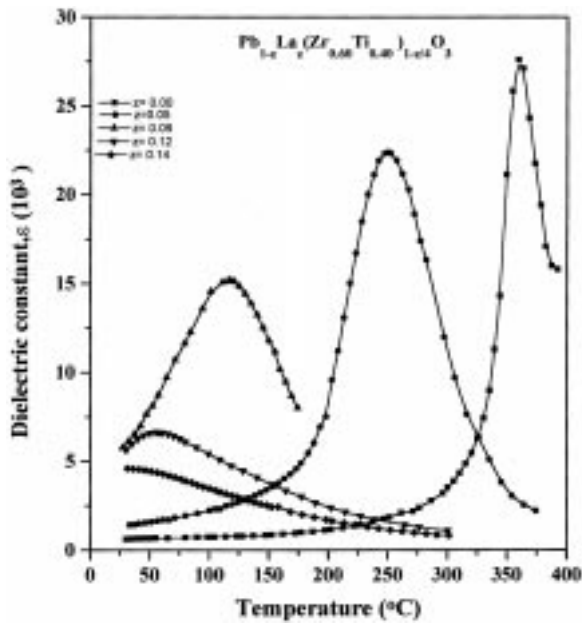

Fig. 6. Variation of dielectric constant (ε) of PLZT with temperature at 10^4 Hz.
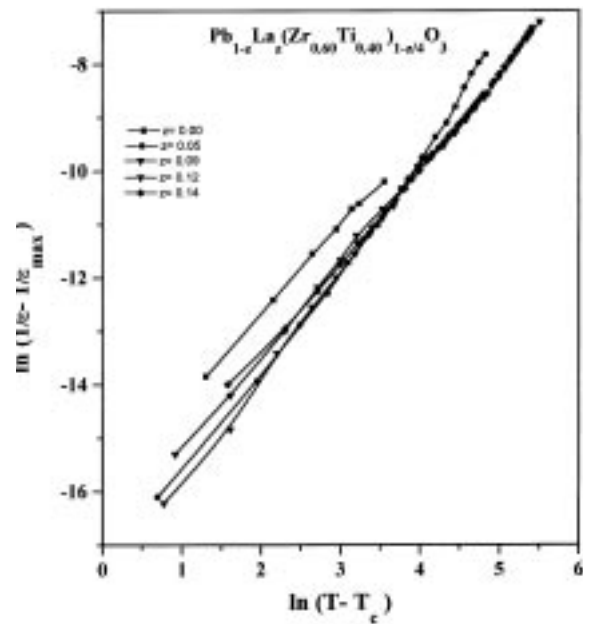

Fig. 8. Variation of $\ln(1/\varepsilon - 1/\varepsilon_{max})$ vs. $\ln(T - T_c)$ of PLZT at 10^4 Hz.

Table 3. Comparison of dielectric parameters of PLZT

z	0.0	0.05	0.09	0.12	0.14
T_c (°C)	359	250	116	55	—
ε_{max} at T_c	27,607	22,349	15,190	6649	—
tanδ at T_c	0.020	0.034	0.037	0.039	—
Diffusivity constant (γ)	1.65	1.74	1.88	1.98	

of temperature on both sides of T_c, except within the range of $\pm$ 20°C around it. As the temperature gradient of the reciprocal of dielectric constant at lower and higher temperatures (ferroelectric and paraelectric phase) is about 2:1 in our experiments, the phase transition of the material is considered to be of second order [13].

Figure 9 shows the hysteresis loops of PLZT at room temperature (30°C). A high electric field (20 kV.cm^{-1}) was required to obtain saturation of polarization. The remanent polarization (P_r) and coercive field (E_c) of PLZT were determined from the hysteresis loops. It is observed that the room temperature hysteresis loops of PLZT for

$z = 0.00 - 0.05$ is of memory-type, which becomes linear-type for $z = 0.09$. This may be the cause of tetragonality in the compound for $z = 0.09$. A mixed-phase (tetragonal + cubic) with very low polarization was observed for $z = 0.12$. A linear P-E graph was observed for $z = 0.14$ indicating the paraelectric phase of the material [14]. The temperature dependence of P_r and E_c of the materials is shown in Fig. 10 and 11 respectively. It is observed that the coercive field (E_c) is approximately a linear function of temperature at the Curie point, whereas polarisation appears to be quadratic, both relations again indicate a second order phase transition in the compounds [13].
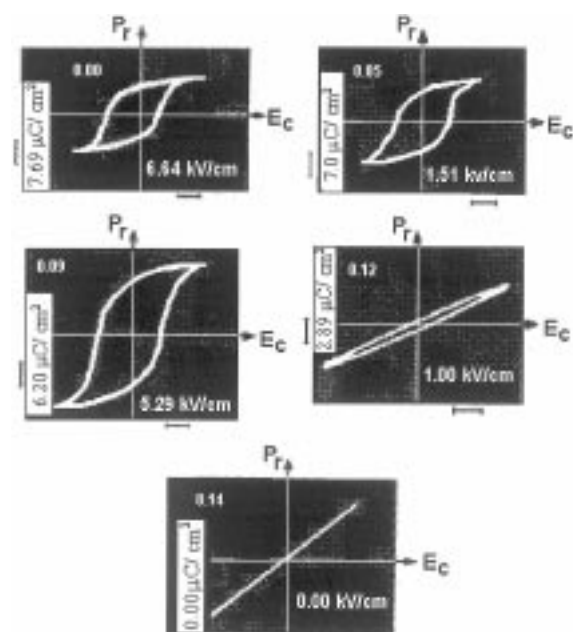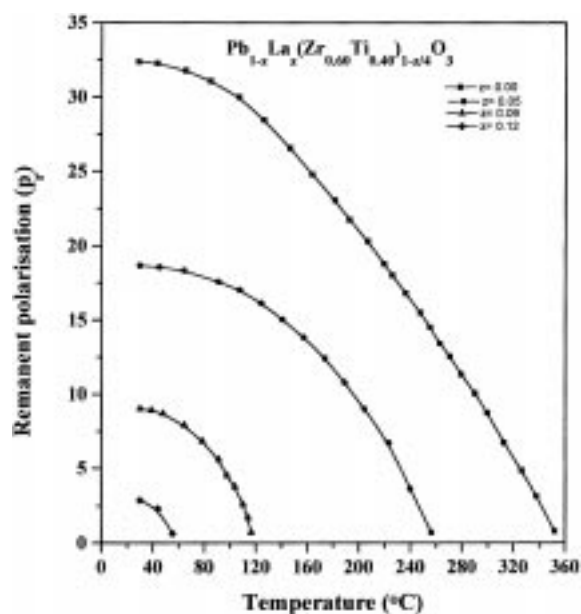

Fig. 9. Room temperature P-E hysteresis loop of PLZT at 50 Hz.

Fig. 10. Temperature dependence of remanent polarisation (P_r) of PLZT at 50 Hz.
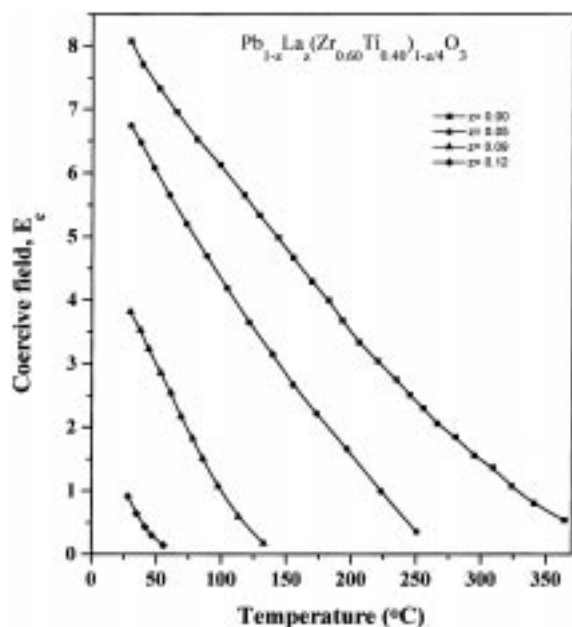
Fig. 11. Temperature dependence of coercive field (E_c) of PLZT at 50 Hz.

4. Conclusion

Sol-gel route of the sample preparation of PLZT at a low temperature ensures a molecular level homogeneity. X-ray diffraction studies confirmed the occurrence of various crystal phases with increase of La^{3+} concentration in PLZT. The density of the samples increases with increasing concentration of La^{3+}. Most of the interplanar d spacings calculated from TEM are comparable to those of XRD. There is a variation in the grain size with the doping concentration of La^{3+}. A significant effect of La concentration on the dielectric and polarisation parameters of PLZT was observed. A diffuse phase transition in PLZT with higher concentration of La was also observed.

References

1. B. Wul and L.M. Goldman, *C.R. Acad. Sci. USSR*, **46**, 123 (1945).
2. K.K. Deb, *Ferroelectrics*, **82**, 45 (1988).
3. Y. Masuda, *Ferroelectrics*, **63**, 261 (1985).
4. R.P. Tandon, R. Singh, R.D.P. Singh, and S. Chandra, *Ferroelectrics*, **120**, 293 (1991).
5. S.T. Liu, J.D. Heaps, and O.N. Tufte, *Ferroelectrics*, **3**, 281 (1971).
6. Y.L. Wang, Z.M. Cheng, Y.R. Sun, and X.-H. Dai, *Physica B*, **150**, 168 (1988).
7. G.H. Haertling, *Am. Ceram. Soc. Bull.*, **46**, 374 (1964).
8. V.A. Isupov, *Ferroelectrics*, **143**, 109 (1993).
9. T.K. Kundu, M. Mukherjee, D. Chakraborty, and T.P. Sinha, *J. Mater. Sci.*, **33**, 1758 (1998).
10. M. Sayer, A. Mansingh, A.K. Arora, and A. Lo, *Integrated Ferroelectrics*, **1**, 129 (1992).
11. S.M. Pilgrim, A.E. Sutherland, and S.R. Winzer, *J. Am. Ceram. Soc.*, **73**, 3122 (1990).
12. C.P. Smith, *Dielectric Behaviour and Structure* (McGraw Hill, New York, 1955).
13. A.J. Moulson and J.M. Herbet, *Electroceramics* (Chapman and Hall, 1990), p. 358.
14. C.D.E. Lakeman and D.A. Payne, *J. Am Ceram. Soc.*, **75**, 3091 (1992).